

# Nickelacyclopentadienylchromium Tricarbonyl Unit as a Bulky Pseudohalogen in Cyclopentadienylchromium Complexes Leading to Low-Energy High-Spin Structures

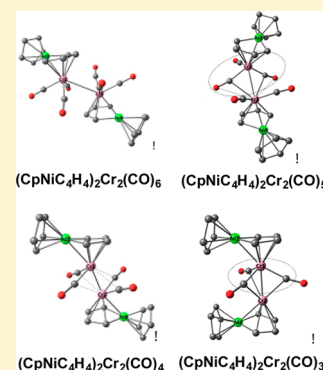
Yi Zeng,<sup>†</sup> Ying Yu,<sup>†</sup> Hao Feng,<sup>\*,†</sup> R. Bruce King,<sup>\*,‡</sup> and Henry F. Schaefer III<sup>‡</sup>

<sup>†</sup>School of Science, Research Center for Advanced Computation, Xihua University, Chengdu, China 610039

<sup>‡</sup>Department of Chemistry and Center for Computational Chemistry, University of Georgia, Athens, Georgia 30602, United States

## Supporting Information

**ABSTRACT:** Recent studies, particularly from the laboratory of Buchalski and co-workers, have resulted in the syntheses of nickelacyclopentadienyl and nickelafuorenyl metallacycles that can function as pentahapto ligands in transition-metal complexes, similar to the ubiquitous cyclopentadienyl ligand. The structures and energetics of the neutral binuclear chromium carbonyls  $(\text{CpNiC}_4\text{H}_4)_2\text{Cr}_2(\text{CO})_n$  ( $n = 6, 5, 4, 3$ ;  $\text{Cp} = \eta^5\text{-C}_5\text{H}_5$ ) containing the unsubstituted nickelacyclopentadienyl ligand have been investigated by density functional theory. The lowest energy  $(\text{CpNiC}_4\text{H}_4)_2\text{Cr}_2(\text{CO})_n$  ( $n = 6, 4$ ) structures are similar to the corresponding experimentally characterized  $\text{Cp}_2\text{Cr}_2(\text{CO})_n$  structures with predicted Cr–Cr distances of  $\sim 3.22$  and  $\sim 2.27$  Å corresponding to the formal single and triple bonds, respectively. This gives the chromium atoms, as well as the nickel atoms, the favored 18-electron configuration. These species appear to be promising synthetic targets. However, the lowest energy  $(\text{CpNiC}_4\text{H}_4)_2\text{Cr}_2(\text{CO})_n$  ( $n = 5, 3$ ) structures, as well as two  $(\text{CpNiC}_4\text{H}_4)_2\text{Cr}_2(\text{CO})_4$  structures  $\sim 10$  to  $12$  kcal/mol in energy above the global minimum, can be dissected into a discrete pseudohalogen  $(\text{CpNiC}_4\text{H}_4)\text{Cr}(\text{CO})_3$  unit and a  $(\text{CpNiC}_4\text{H}_4)\text{Cr}(\text{CO})_{n-3}$  unit linked by a Cr–Cr bond flanked by one to three generally weakly semibridging CO groups. In most cases, the chromium atoms in the  $(\text{CpNiC}_4\text{H}_4)\text{Cr}(\text{CO})_{n-3}$  units of these structures have 14–16-electron configurations rather than the favored 18-electron configuration. This leads to triplet and even quintet spin states in the lowest energy structures.



## 1. INTRODUCTION

The chemistry of the cyclopentadienylmetal carbonyls of the group 6 metals (Cr, Mo, W) dates back to the 1955 discovery of the reaction of the cyclopentadienide anion with  $\text{M}(\text{CO})_6$  to displace three CO groups to give the anions  $[\text{CpM}(\text{CO})_3]^-$  ( $\text{Cp} = \eta^5\text{-C}_5\text{H}_5$ ).<sup>1,2</sup> Mild oxidation of the anions or the conjugate acids  $\text{CpM}(\text{CO})_3\text{H}$  then gives the corresponding  $\text{Cp}_2\text{M}_2(\text{CO})_6$  dimers (Figure 1). The molybdenum compound  $\text{Cp}_2\text{Mo}_2(\text{CO})_6$  was also obtained independently from the thermal reaction of  $\text{Mo}(\text{CO})_6$  with dicyclopentadiene.<sup>3</sup>

The binuclear cyclopentadienylmetal carbonyls of the group 6 metals were subsequently found to provide the first examples of metal–metal multiple bonds in metal carbonyl chemistry. Such compounds date back to 1967 when King and Bisnette<sup>4</sup> reported the thermal reaction of  $\text{Mo}(\text{CO})_6$  with pentam-

ethylcyclopentadiene to give the tetracarbonyl  $(\eta^5\text{-Me}_5\text{C}_5)_2\text{Mo}_2(\text{CO})_4$ , rather than the expected hexacarbonyl  $(\eta^5\text{-Me}_5\text{C}_5)_2\text{Mo}_2(\text{CO})_6$  analogous to the unsubstituted cyclopentadienyl derivative. An X-ray structural determination on  $(\eta^5\text{-Me}_5\text{C}_5)_2\text{Mo}_2(\text{CO})_4$  showed a short  $\text{Mo}\equiv\text{Mo}$  distance of 2.488 Å compared with 3.235 Å for  $\text{Cp}_2\text{Mo}_2(\text{CO})_6$ , which clearly indicates a  $\text{Mo}\equiv\text{Mo}$  single bond.<sup>5</sup> Considering the  $\text{Mo}\equiv\text{Mo}$  bond in  $\text{Cp}_2\text{Mo}_2(\text{CO})_4$  as a formal triple bond gives each molybdenum the favored 18-electron configuration. Subsequently, the analogous chromium compounds  $(\eta^5\text{-R}_5\text{C}_5)_2\text{Cr}_2(\text{CO})_4$  ( $\text{R} = \text{H},^6 \text{Me}^{7,8}$ ) were also synthesized and likewise found to have relatively short  $\text{Cr}\equiv\text{Cr}$  distances around 2.24 Å, suggesting similar formal triple bonds (Figure 1).

Recently, Buchalski and co-workers<sup>9–13</sup> showed that one of the CH vertices in the cyclopentadienide anion could be replaced by an isoelectronic and isolobal  $\text{CpNi}$  vertex. They used the related nickelafuorenyl (nickeladibenzocyclopentadienide) anion to synthesize the sandwich compounds  $(\eta^5\text{-CpNiC}_{12}\text{H}_8)_2\text{M}$  ( $\text{M} = \text{Co}, \text{Ni}$ ) with cobalt and nickel as central atoms. The perphenylated nickelacyclopentadienide anion  $\text{CpNiC}_4\text{Ph}_4^-$  was also prepared and used to synthesize a ferrocene analogue,  $[\text{CpNiC}_4\text{Ph}_4]\text{FeCp}$ , in which one of the

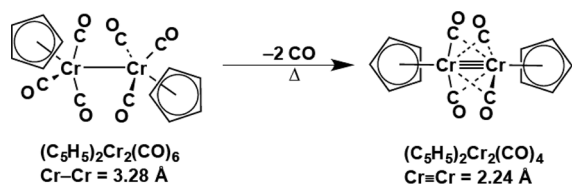


**Figure 1.** Cyclopentadienylchromium carbonyls  $\text{Cp}_2\text{Cr}_2(\text{CO})_n$  ( $n = 6, 4$ ).

**Received:** February 13, 2015

**Published:** May 15, 2015



CH groups in tetraphenylferrocene is replaced by a CpNi unit.<sup>14</sup> These nickelacyclopentadienide and nickelafuorenyd anions are feasible reagents to synthesize the heterobimetallic anions  $[(\text{CpNiC}_4\text{H}_8)\text{M}(\text{CO})_3]^-$  and  $[(\text{CpNiC}_4\text{Ph}_4)\text{M}(\text{CO})_3]^-$  ( $\text{M} = \text{Cr}, \text{Mo}, \text{W}$ ), which can then be oxidized to the corresponding neutral species (Figure 2).

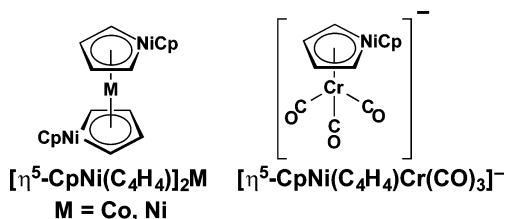


**Figure 2.** Pentahapto  $\eta^5\text{-CpNiC}_4\text{H}_4$  ( $\text{Cp} = \eta^5\text{-C}_5\text{H}_5$ ) ligand in metallocene and chromium carbonyl chemistry.

We now report a density functional study on the neutral binuclear chromium carbonyl complexes  $(\text{CpNiC}_4\text{H}_4)_2\text{Cr}_2(\text{CO})_n$  ( $n = 6, 5, 4, 3$ ). The lowest energy structures were found to have features different from those of the corresponding  $\text{Cp}_2\text{Cr}_2(\text{CO})_n$  derivatives. More specifically, many of the lowest energy  $(\text{CpNiC}_4\text{H}_4)_2\text{Cr}_2(\text{CO})_n$  structures have a distinct  $\text{CpNiC}_4\text{H}_4\text{Cr}(\text{CO})_3$  unit linked through the remaining  $\text{CpNiC}_4\text{H}_4\text{Cr}(\text{CO})_n$  ( $n = 3, 2, 1$ ) portion of the molecule by a Cr–Cr single bond. The  $\text{CpNiC}_4\text{H}_4\text{Cr}(\text{CO})_3$  unit can be considered to be a bulky pseudohalogen. Thus, the  $(\text{CpNiC}_4\text{H}_4)_2\text{Cr}_2(\text{CO})_n$  structures containing such a pseudohalogen  $\text{CpNiC}_4\text{H}_4\text{Cr}(\text{CO})_3$  structural unit may be considered as analogues of  $\text{CpCr}(\text{CO})_n\text{Cl}$  ( $n = 2, 1$ ) with 16- and 14-electron configurations, respectively, for the central chromium atom corresponding to triplet and quintet spin states, respectively.

## 2. THEORETICAL METHODS

Computational methods have become an integral part of organometallic chemistry.<sup>15–21</sup> Two density functional theory (DFT) methods were used in this work. The BP86 method combines Becke's 1988 exchange functional (B) with Perdew's 1986 gradient-corrected correlation functional (P86)<sup>22,23</sup> and usually provides better vibrational frequencies.<sup>24,25</sup> The second functional is a meta-GGA DFT method, M06-L, developed by Truhlar and Zhao.<sup>26</sup> They suggest M06-L for transition-metal compounds, since it predicts relative energies closer to experimental values. Thus, we adopt the energy orderings predicted by the M06-L method, but list the results from the BP86 method in the Supporting Information.

Standard double- $\zeta$  plus polarization (DZP) basis sets were adopted. For hydrogen, a set of p polarization functions  $\alpha_p(\text{H}) = 0.75$  is added to the Huzinaga–Dunning DZ sets. For carbon and oxygen, one set of pure spherical harmonic d functions with orbital exponents  $\alpha_d(\text{C}) = 0.75$  and  $\alpha_d(\text{O}) = 0.85$  is added to the Huzinaga–Dunning standard contracted DZ sets.<sup>27,28</sup> For Cr and Ni, our loosely contracted DZP basis set, derived from the Wachters primitive set,<sup>29</sup> is used after being augmented by two sets of p functions and one set of d functions and then contracted using the method of Hood, Pitzer, and Schaefer.<sup>30</sup> These DZP basis sets are designated as (4s1p/2s1p) for hydrogen, (9s5p1d/4s2p1d) for carbon and oxygen, and (14s11p6d/10s8p3d) for Cr and Ni.

The Gaussian 09 software was used for the structural optimizations.<sup>31</sup> Vibrational frequencies were determined by evaluating analytically the second derivatives of the energy with respect to the nuclear coordinates. The ultrafine grid, i.e., the pruned (99, 590) grid, was used for the computation of two-electron integrals.<sup>32</sup> Natural bond orbital (NBO) analyses<sup>33–35</sup> were carried out using the DZP M06-L

method to provide information on the chemical bonding in these systems.

## 3. RESULTS

All of the  $(\text{CpNiC}_4\text{H}_4)_2\text{Cr}_2(\text{CO})_n$  ( $n = 6, 5, 4, 3$ ) structures found in this work are predicted to have Ni–Cr distances of  $\sim 2.4$  Å (Figures 3–6). These Ni–Cr distances, in concert with the Wiberg bond indices (WBIs) of 0.07–0.27 (Table 1), suggest formal Ni–Cr single bonds, thereby giving each nickel atom the favored 18-electron configuration.

**3.1. Saturated  $(\text{CpNiC}_4\text{H}_4)_2\text{Cr}_2(\text{CO})_6$  Structures.** The saturated  $(\text{CpNiC}_4\text{H}_4)_2\text{Cr}_2(\text{CO})_6$  structures are derived from the experimentally known  $\text{Cp}_2\text{Cr}_2(\text{CO})_6$  structure by replacing a CH unit in each Cp ring with a CpNi unit (Figure 3). Thus,

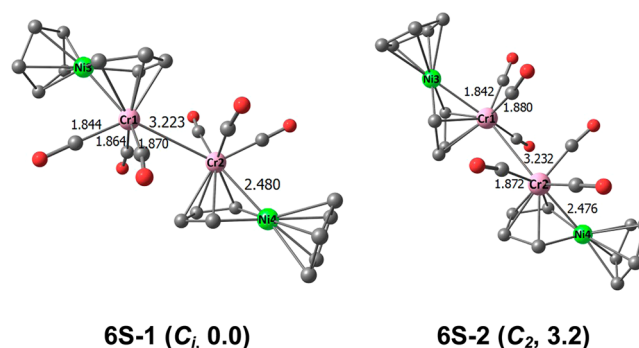


**Figure 3.** Equilibrium geometries and relative energies (kcal/mol) for the two  $(\text{CpNiC}_4\text{H}_4)_2\text{Cr}_2(\text{CO})_6$  structures (hydrogens omitted for clarity).

two low-lying singlet  $(\text{CpNiC}_4\text{H}_4)_2\text{Cr}_2(\text{CO})_6$  structures, namely, unbridged *trans*-6S-1 and *cis*-6S-2, are found with energies within 3.2 kcal/mol, suggesting a fluxional system. Triplet  $(\text{CpNiC}_4\text{H}_4)_2\text{Cr}_2(\text{CO})_6$  structures are relatively high energy structures, lying 12 kcal/mol above the singlet structures, and thus are not discussed in this paper.

The *trans*- $(\text{CpNiC}_4\text{H}_4)_2\text{Cr}_2(\text{CO})_6$  structure 6S-1 is predicted to lie 3.2 kcal/mol lower in energy than the *cis* structure 6S-2 (Figure 3). The predicted Cr–Cr distances in 6S-1 and 6S-2 of 3.223 and 3.232 Å, respectively, are reasonably close to the experimental Cr–Cr bond distance of 3.281 Å in  $\text{Cp}_2\text{Cr}_2(\text{CO})_6$  as determined by X-ray crystallography.<sup>36</sup> These Cr–Cr distances in 6S-1 and 6S-2 coupled with their WBIs of 0.23 and 0.24 suggest formal single bonds, thereby giving each chromium atom the favored 18-electron configuration.

**3.2. Unsaturated  $(\text{CpNiC}_4\text{H}_4)_2\text{Cr}_2(\text{CO})_n$  Structures ( $n = 5, 4, 3$ ).** **3.2.1.  $(\text{CpNiC}_4\text{H}_4)_2\text{Cr}_2(\text{CO})_5$ .** The triplet  $(\text{CpNiC}_4\text{H}_4)_2\text{Cr}_2(\mu\text{-CO})_2(\text{CO})_3$  structure 5T-1 is found to be the lowest energy structure (Figure 4). Quintet  $(\text{CpNiC}_4\text{H}_4)_2\text{Cr}_2(\text{CO})_5$  structures are relatively high energy structures, lying 26 kcal/mol above 5T-1, and thus are not discussed in this paper. Structure 5T-1 can be dissected into a  $(\text{CpNiC}_4\text{H}_4)\text{Cr}(\text{CO})_3$  unit similar to half of 6S-1 or 6S-2 bonded to a  $(\text{CpNiC}_4\text{H}_4)\text{-Cr}(\text{CO})_2$  unit. However, two of the carbonyl groups in the  $(\text{CpNiC}_4\text{H}_4)\text{Cr}(\text{CO})_3$  unit become weakly semibridging CO groups to the  $(\text{CpNiC}_4\text{H}_4)\text{Cr}(\text{CO})_2$  unit. These semibridging CO groups have short Cr–C distances of 1.871 and 1.862 Å and long Cr–C distances of 2.484 and 2.630 Å. The Cr–Cr distance in 5T-1 of 2.738 Å is  $\sim 0.5$  Å shorter than the Cr–Cr single bond distances in 6S-1 or 6S-2 and on this basis might be considered to be a formal double bond. However, its WBI of only 0.27 in 5T-1 is close to the WBIs of 0.23 and 0.24 for the

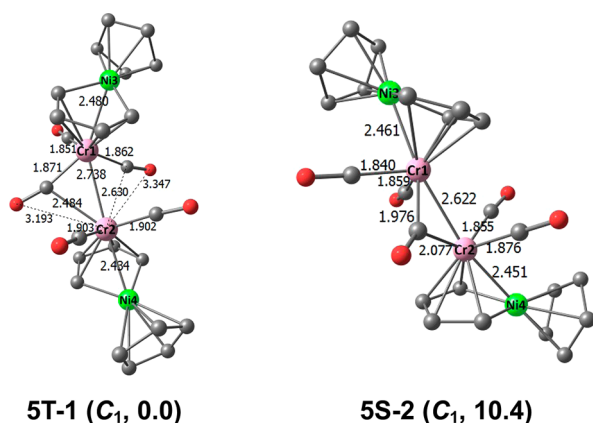


**Figure 4.** Equilibrium geometries and relative energies (kcal/mol) for the two  $(\text{CpNiC}_4\text{H}_4)_2\text{Cr}_2(\text{CO})_5$  structures.

Cr–Cr single bonds in 6S-1 or 6S-2. Considering the Cr–Cr bond in 5T-1 as a formal single bond gives the chromium bearing three CO groups the favored 18-electron configuration but the chromium bearing only two CO groups a 16-electron configuration. The localization of the spin density on the latter chromium atom (Figure S1, Supporting Information) supports this interpretation of the Cr–Cr bonding.

The lowest energy singlet  $(\text{CpNiC}_4\text{H}_4)_2\text{Cr}_2(\mu\text{-CO})(\text{CO})_4$  structure 5S-2, lying 10.4 kcal/mol in energy above 5T-1, has a single CO bridge. The Cr=Cr distance of 2.622 Å in 5S-2 is  $\sim 0.6$  Å shorter than the formal Cr–Cr single bonds in 6S-1 and 6S-2 and 0.12 Å shorter than the Cr–Cr bond in 5T-1. This coupled with the 0.52 WBI value for 5S-2, which is approximately twice the WBIs for 6S-1, 6S-2, and 5T-1, suggests a formal double bond in 5S-2, thereby giving each chromium atom the favored 18-electron configuration.

**3.2.2.  $(\text{CpNiC}_4\text{H}_4)_2\text{Cr}_2(\text{CO})_4$ .** The three lowest energy  $(\text{CpNiC}_4\text{H}_4)_2\text{Cr}_2(\text{CO})_4$  structures include one singlet structure (4S-1), one quintet structure (4Q-2), and one triplet structure (4T-3) (Figure 5). The  $C_{2h}$  semibridged singlet structure 4S-1 is predicted to be the global minimum. The very short Cr≡Cr distance of 2.265 Å in 4S-1 combined with a relatively large WBI of 0.83 suggests a formal triple bond, thereby giving each chromium atom the favored 18-electron configuration. This Cr≡Cr distance in 4S-1 is very similar to the experimental Cr≡Cr distances of  $\sim 2.24$  Å in the cyclopentadienyl derivatives  $(\eta^5\text{-R}_5\text{C}_5)_2\text{Cr}_2(\text{CO})_4$  ( $\text{R} = \text{H}$ ,<sup>6</sup>  $\text{Me}$ ,<sup>7,8</sup>), further

supporting the interpretation of the Cr≡Cr interaction in 4S-1 as a formal triple bond.

The doubly bridged quintet 4Q-2 and triplet 4T-3 are both higher energy  $(\text{CpNiC}_4\text{H}_4)_2\text{Cr}_2(\mu\text{-CO})_2(\text{CO})_2$  structures, lying 10.0 and 12.6 kcal/mol, respectively, above 4S-1 (Figure 5). The Cr–Cr distance of 2.704 Å in 4Q-2 coupled with the WBI of 0.22 can be interpreted as a formal single bond, providing Cr1 with the favored 18-electron configuration but Cr2 with only a 14-electron configuration. The shorter Cr=Cr distance of 2.582 Å in 4T-3 corresponding to a WBI value of 0.32 can be interpreted as a formal double bond. This gives Cr1 the favored 18-electron configuration with a formal negative charge but Cr2 only a 16-electron configuration with a positive formal charge. The spin densities of 4Q-2 and 4T-3 locate the four and two unpaired electrons on the Cr2 atoms with 14- and 16-electron configurations, respectively (Figure S2, Supporting Information).

**3.2.3.  $(\text{CpNiC}_4\text{H}_4)_2\text{Cr}_2(\text{CO})_3$ .** Three low-lying triply bridged  $(\text{CpNiC}_4\text{H}_4)_2\text{Cr}_2(\mu\text{-CO})_3$  structures are found to be genuine minima with  $C_s$  symmetry (Figure 6). The quintet  $(\text{CpNiC}_4\text{H}_4)_2\text{Cr}_2(\mu\text{-CO})_3$  structure 3Q-1 is the global minimum. It has three semibridging carbonyl groups with short Cr–C distances of 1.857 and 1.892 Å and long Cr–C distances of 2.263 and 2.455 Å. The predicted Cr=Cr distance of 2.516 Å and its WBI of 0.28 suggest a weak formal double bond. This gives Cr1 the favored 18-electron configuration with a formal negative charge. However, the Cr2 atom has only a 14-electron configuration, even with a formal positive charge. The spin density of 3Q-1 (Figure S3, Supporting Information) indicates that the four unpaired electrons of the quintet spin state are mostly localized on the Cr2 atom, consistent with its 14-electron configuration.

The triplet and singlet  $(\text{CpNiC}_4\text{H}_4)_2\text{Cr}_2(\mu\text{-CO})_3$  structures 3T-2 and 3S-3, lying 7.6 and 24.2 kcal/mol in energy, respectively, above 3Q-1, have three semibridging carbonyl groups, with short Cr–C distances of  $\sim 1.9$  Å and long Cr–C distances of  $\sim 2.3$  Å (Figure 6). The predicted Cr=Cr distances of 2.397 and 2.332 Å in 3T-2 and 3S-3, respectively, are shorter than that in 3Q-1. However, the WBIs of 0.39 and 0.50 for 3T-2 and 3S-3, respectively, similar to the WBI of 0.52 for the  $(\text{CpNiC}_4\text{H}_4)_2\text{Cr}_2(\mu\text{-CO})(\text{CO})_4$  structure 5S-2, suggest formal Cr=Cr double bonds in these structures. This gives the Cr1 atoms in these structures the favored 18-electron configuration with a formal negative charge. However, the Cr2 atoms in 3T-2 and 3S-3 have only 14-electron configurations with formal positive charges. The spin density

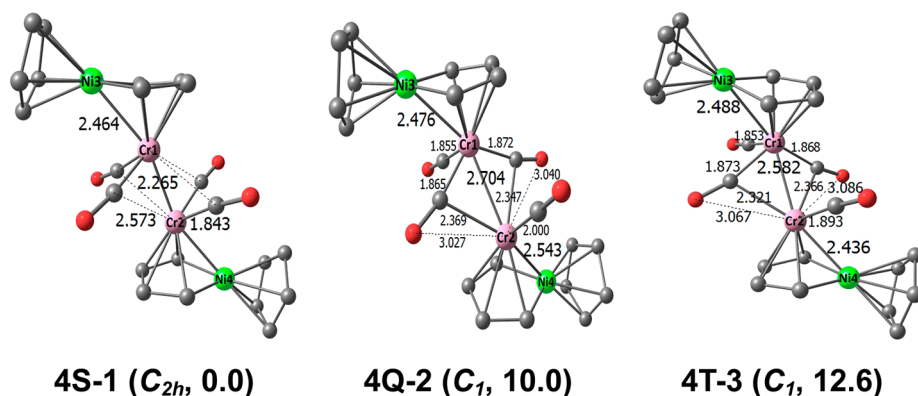


**Figure 5.** Equilibrium geometries and relative energies (kcal/mol) for the three  $(\text{CpNiC}_4\text{H}_4)_2\text{Cr}_2(\text{CO})_4$  structures.



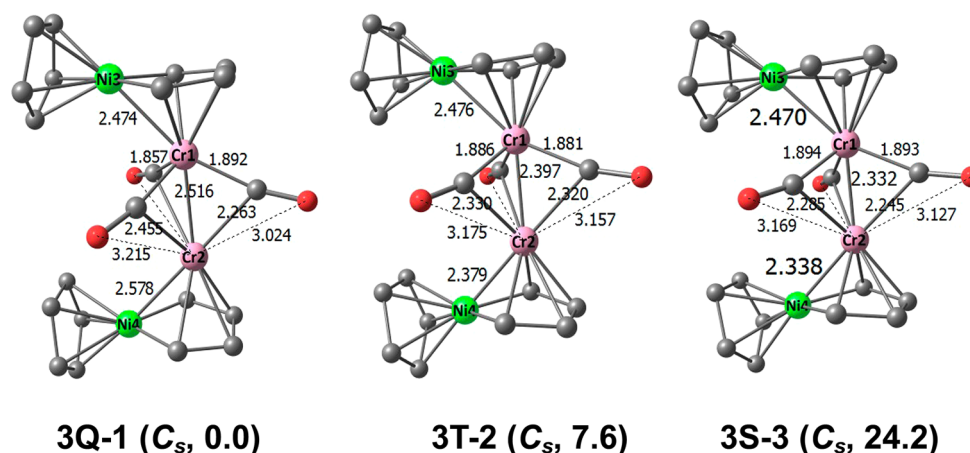


Figure 6. Equilibrium geometries and relative energies (kcal/mol) for the three  $(\text{CpNiC}_4\text{H}_4)_2\text{Cr}_2(\text{CO})_3$  structures.

Table 1. Metal–Metal Distances, Natural Population Analysis Natural Charges, Metal Electron Configurations, Formal Metal–Metal Bond Orders, and WBIs for the  $(\text{CpNiC}_4\text{H}_4)_2\text{Cr}_2(\text{CO})_n$  ( $n = 6, 5, 4, 3$ ) Structures Using the M06-L Method<sup>a</sup>

		6S-1, C <sub>i</sub>	6S-2, C <sub>2</sub>	5T-1, C <sub>i</sub>	5S-2, C <sub>i</sub>	4S-1, C <sub>2h</sub>	4Q-2, C <sub>i</sub>	4T-3, C <sub>i</sub>	3Q-1, C <sub>s</sub>	3T-2, C <sub>s</sub>	3S-3, C <sub>s</sub>
metal–metal distance	Cr1–Cr2	<b>3.223</b>	3.232	<b>2.738</b>	2.622	<b>2.265</b>	2.704	2.582	<b>2.516</b>	2.397	2.332
	Ni3–Cr1	<b>2.480</b>	2.476	<b>2.480</b>	2.461	<b>2.464</b>	2.476	2.488	<b>2.474</b>	2.476	2.470
	Ni4–Cr2	<b>2.480</b>	2.476	<b>2.434</b>	2.451	<b>2.464</b>	2.543	2.436	<b>2.578</b>	2.379	2.338
metal natural charge	Cr1	<b>−0.60</b>	−0.58	<b>−0.63</b>	−0.45	<b>−0.36</b>	−0.62	−0.64	<b>−0.61</b>	−0.57	−0.53
	Cr2	<b>−0.60</b>	−0.58	<b>−0.14</b>	−0.42	<b>−0.36</b>	0.51	0.21	<b>0.74</b>	0.38	0.20
	Ni3	<b>0.77</b>	0.77	<b>0.76</b>	0.77	<b>0.77</b>	0.75	0.75	<b>0.75</b>	0.75	0.75
	Ni4	<b>0.77</b>	0.77	<b>0.76</b>	0.77	<b>0.77</b>	0.70	0.75	<b>0.70</b>	0.75	0.77
metal electron configuration	Cr1	<b>18</b>	18	<b>18</b>	18	<b>18</b>	18	18	<b>18</b>	18	18
	Cr2	<b>18</b>	18	<b>16</b>	18	<b>18</b>	14	16	<b>14</b>	14	14
	Ni3	<b>18</b>	18	<b>18</b>	18	<b>18</b>	18	18	<b>18</b>	18	18
	Ni4	<b>18</b>	18	<b>18</b>	18	<b>18</b>	18	18	<b>18</b>	18	18
formal bond order	Cr1–Cr2	<b>1</b>	1	<b>1</b>	2	<b>3</b>	1	2	<b>2</b>	2	2
	Ni3–Cr1	<b>1</b>	1	<b>1</b>	1	<b>1</b>	1	1	<b>1</b>	1	1
	Ni4–Cr2	<b>1</b>	1	<b>1</b>	1	<b>1</b>	1	1	<b>1</b>	1	1
Wiberg bond index	Cr1–Cr2	<b>0.23</b>	0.24	<b>0.27</b>	0.52	<b>0.83</b>	0.22	0.32	<b>0.28</b>	0.39	0.50
	Ni3–Cr1	<b>0.17</b>	0.18	<b>0.16</b>	0.21	<b>0.18</b>	0.17	0.16	<b>0.17</b>	0.17	0.17
	Ni4–Cr2	<b>0.17</b>	0.18	<b>0.19</b>	0.19	<b>0.18</b>	0.10	0.21	<b>0.07</b>	0.25	0.27

<sup>a</sup>Values for global minimum structures are shown in bold type.

of the two unpaired electrons in 3T-2 (Figure S3, Supporting Information) is mainly localized on the Cr2 atom, consistent with this interpretation.

**3.3. NBO Analysis.** Table 1 lists the Ni–Cr and Cr–Cr distances, the formal Ni–Cr and Cr–Cr bond orders, the natural charges on the Ni and Cr atoms, and the electron configurations of the Ni and Cr atoms for all of the structures reported in this research. In general, an increase in the Cr–C distances between the Cr2 atoms and the semibridging carbonyl groups increases the positive natural charge of the Cr2 atoms compared with the Cr1 atoms, since increased electron density arising from  $\sigma$ -donation from the CO groups to the Cr–Cr atom is not completely balanced by  $\pi$  back-bonding from the chromium atom to the CO  $\pi^*$  antibonding orbitals. For the  $(\text{CpNiC}_4\text{H}_4)_2\text{Cr}_2(\text{CO})_5$  structure 5T-1, the Cr2 atom with long Cr–C distances (2.484 and 2.630 Å) has a smaller NBO negative charge of  $-0.14$  relative to the  $-0.63$  negative charge on the Cr1 atom. Similarly, in the  $(\text{CpNiC}_4\text{H}_4)_2\text{Cr}_2(\text{CO})_4$  and  $(\text{CpNiC}_4\text{H}_4)_2\text{Cr}_2(\text{CO})_3$  structures 4Q-2, 4T-3, 3Q-1, 3T-2, and 3S-3, the Cr2 atoms have positive charges ranging from 0.20 to 0.74 compared with the negative charges ranging from  $-0.53$  to  $-0.64$  for Cr1.

The WBIs in Table 1 of the Ni–Cr and Cr–Cr bonds for the singlet  $(\text{CpNiC}_4\text{H}_4)_2\text{Cr}_2(\text{CO})_n$  structures are shown to correlate with the formal bond orders suggested by the Ni–Cr and Cr–Cr distances and electron counting except for some of the higher spin state triplet and quintet structures suggested to have Cr–Cr multiple bonds such as 4T-3 and 3T-2. The correlation between WBIs and formal bond orders for the triplet and quintet  $(\text{CpNiC}_4\text{H}_4)_2\text{Cr}_2(\text{CO})_n$  structures is not as good, in accord with past experience. Thus, for the Ni–Cr single bonds the WBIs range from 0.07 to 0.27. Similarly, the WBIs for the Cr–Cr single bonds range from 0.22 to 0.27. The WBIs for the Cr=Cr double bonds in 5S-2, 3T-2, and 3S-3 are significantly higher, ranging from 0.39 to 0.52. The still higher WBI value of 0.83 for 4S-1 can be interpreted as indicating a strong formal Cr≡Cr triple bond. These WBI values are consistent with those in our previous theoretical studies<sup>37</sup> where formal Fe–Fe single bonds were found to have values of 0.12–0.19.

**3.4. Vibrational Frequencies.** Table 2 exhibits the harmonic  $\nu(\text{CO})$  frequencies and their infrared intensities for all of the  $(\text{CpNiC}_4\text{H}_4)_2\text{Cr}_2(\text{CO})_n$  ( $n = 6, 5, 4, 3$ ) structures. These were obtained by the BP86 method, which has been

**Table 2.**  $\nu(\text{CO})$  Frequencies ( $\text{cm}^{-1}$ ) and IR Intensities ( $\text{km/mol}$ ) in Parentheses for the  $(\text{CpNiC}_4\text{H}_4)_2\text{Cr}_2(\text{CO})_n$  Structures Using the BP86 Method<sup>a</sup>

6S-1	$\text{C}_i$	1878 ( <i>A<sub>g</sub></i> , 0), 1896 ( <i>A<sub>u</sub></i> , 218), 1908 ( <i>A<sub>u</sub></i> , 1350), 1908 ( <i>A<sub>g</sub></i> , 0), 1932 ( <i>A<sub>u</sub></i> , 1694), 1959 ( <i>A<sub>g</sub></i> , 0)
6S-2	$\text{C}_2$	1883 ( <i>A</i> , 274), 1886 ( <i>B</i> , 521), 1918 ( <i>A</i> , 8), 1923 ( <i>B</i> , 874), 1935 ( <i>B</i> , 646), 1977 ( <i>A</i> , 792)
5T-1	$\text{C}_1$	1828 ( <i>A</i> , 435), 1875 ( <i>A</i> , 132), 1912 ( <i>A</i> , 722), 1920 ( <i>A</i> , 1387), 1946 ( <i>A</i> , 26)
5S-2	$\text{C}_2$	<b>1746</b> ( <i>A</i> , 401), 1885 ( <i>B</i> , 67), 1913 ( <i>A</i> , 780), 1932 ( <i>B</i> , 1184), 1951 ( <i>A</i> , 91)
4S-1	$\text{C}_{2h}$	1878 ( <i>B<sub>g</sub></i> , 0), 1889 ( <i>A<sub>u</sub></i> , 1030), 1902 ( <i>B<sub>u</sub></i> , 808), 1925 ( <i>A<sub>g</sub></i> , 0)
4Q-2	$\text{C}_1$	1798 ( <i>A</i> , 605), 1819 ( <i>A</i> , 87), 1916 ( <i>A</i> , 1086), 1950 ( <i>A</i> , 292)
4T-3	$\text{C}_1$	1818 ( <i>A</i> , 607), 1843 ( <i>A</i> , 150), 1896 ( <i>A</i> , 793), 1935 ( <i>A</i> , 569)
3Q-1	$\text{C}_s$	1801 ( <i>A'</i> , 750), 1839 ( <i>A'</i> , 565), 1873 ( <i>A'</i> , 33)
3T-2	$\text{C}_s$	1826 ( <i>A'</i> , 764), 1842 ( <i>A''</i> , 625), 1876 ( <i>A'</i> , 13)
3S-3	$\text{C}_s$	1815 ( <i>A'</i> , 791), 1839 ( <i>A''</i> , 636), 1868 ( <i>A'</i> , 5)

<sup>a</sup>Bridging  $\nu(\text{CO})$  frequencies are given in bold type, whereas weakly semibridging  $\nu(\text{CO})$  frequencies are given in italic type.

shown to predict  $\nu(\text{CO})$  frequencies closer to the experimental fundamental frequencies.<sup>38,39</sup> The fully terminal  $\nu(\text{CO})$  frequencies range from 1885 to 1977  $\text{cm}^{-1}$ , whereas the weakly semibridging  $\nu(\text{CO})$  frequencies are typically somewhat lower from 1798 to 1925  $\text{cm}^{-1}$  and generally decrease upon shortening the long Cr–C bond, approaching a more nearly symmetrical bridging CO group. The symmetrical bridging  $\nu(\text{CO})$  frequency in 5S-2 is distinctly even lower at 1746  $\text{cm}^{-1}$ . The significantly lower  $\nu(\text{CO})$  frequencies for bridging relative to terminal CO groups are consistent with the longer C–O distances and correspondingly lower effective C–O bond orders in bridging CO groups relative to terminal CO groups.

**3.5. Thermochemistry.** The thermochemical predictions in Tables 3 and 4 provide insights into the viability of the

**Table 3.** Dissociation Energies (kcal/mol) for the Successive Removal of Carbonyl Groups from  $(\text{CpNiC}_4\text{H}_4)_2\text{Cr}_2(\text{CO})_n$  by the M06-L Method

$(\text{CpNiC}_4\text{H}_4)_2\text{Cr}_2(\text{CO})_6$ (6S-1) $\rightarrow$ $(\text{CpNiC}_4\text{H}_4)_2\text{Cr}_2(\text{CO})_5$ (5T-1) + CO	23.1
$(\text{CpNiC}_4\text{H}_4)_2\text{Cr}_2(\text{CO})_5$ (5T-1) $\rightarrow$ $(\text{CpNiC}_4\text{H}_4)_2\text{Cr}_2(\text{CO})_4$ (4S-1) + CO	19.1
$(\text{CpNiC}_4\text{H}_4)_2\text{Cr}_2(\text{CO})_4$ (4S-1) $\rightarrow$ $(\text{CpNiC}_4\text{H}_4)_2\text{Cr}_2(\text{CO})_3$ (3Q-1) + CO	29.8

**Table 4.** Energies (kcal/mol) for the Disproportionation Reactions  $2(\text{CpNiC}_4\text{H}_4)_2\text{Cr}_2(\text{CO})_n \rightarrow (\text{CpNiC}_4\text{H}_4)_2\text{Cr}_2(\text{CO})_{n+1} + (\text{CpNiC}_4\text{H}_4)_2\text{Cr}_2(\text{CO})_{n-1}$  by the M06-L Method

$2(\text{CpNiC}_4\text{H}_4)_2\text{Cr}_2(\text{CO})_5$ (5T-1) $\rightarrow$ $(\text{CpNiC}_4\text{H}_4)_2\text{Cr}_2(\text{CO})_6$ (6S-1) + $(\text{CpNiC}_4\text{H}_4)_2\text{Cr}_2(\text{CO})_4$ (4S-1)	−4.0
$2(\text{CpNiC}_4\text{H}_4)_2\text{Cr}_2(\text{CO})_4$ (4S-1) $\rightarrow$ $(\text{CpNiC}_4\text{H}_4)_2\text{Cr}_2(\text{CO})_5$ (5T-1) + $(\text{CpNiC}_4\text{H}_4)_2\text{Cr}_2(\text{CO})_3$ (3Q-1)	10.7

$(\text{CpNiC}_4\text{H}_4)_2\text{Cr}_2(\text{CO})_n$  derivatives. Noteworthy are the dissociation energies (Table 3) for the single carbonyl dissociation steps  $(\text{CpNiC}_4\text{H}_4)_2\text{Cr}_2(\text{CO})_n \rightarrow (\text{CpNiC}_4\text{H}_4)_2\text{Cr}_2(\text{CO})_{n-1} + \text{CO}$  and the disproportionation reactions  $2(\text{CpNiC}_4\text{H}_4)_2\text{Cr}_2(\text{CO})_n \rightarrow (\text{CpNiC}_4\text{H}_4)_2\text{Cr}_2(\text{CO})_{n+1} + (\text{CpNiC}_4\text{H}_4)_2\text{Cr}_2(\text{CO})_{n-1}$  (Table 4) considering only the lowest energy structures.

The thermochemistry of the  $(\text{CpNiC}_4\text{H}_4)_2\text{Cr}_2(\text{CO})_n$  system suggests that the singlet semibridged  $(\text{CpNiC}_4\text{H}_4)_2\text{Cr}_2(\text{CO})_4$

structure 4S-1 is a viable synthetic objective. Thus, the predicted carbonyl dissociation energy of 19.1 kcal/mol required to go from  $(\text{CpNiC}_4\text{H}_4)_2\text{Cr}_2(\text{CO})_5$  (5T-1) to  $(\text{CpNiC}_4\text{H}_4)_2\text{Cr}_2(\text{CO})_4$  (4S-1) is much smaller than the 29.8 kcal/mol energy required to go from  $(\text{CpNiC}_4\text{H}_4)_2\text{Cr}_2(\text{CO})_4$  (4S-1) to  $(\text{CpNiC}_4\text{H}_4)_2\text{Cr}_2(\text{CO})_3$  (3Q-1) (Table 3). The latter dissociation energy approaches the experimental CO dissociation energy of 37 kcal/mol for the very stable simple metal carbonyl  $\text{Cr}(\text{CO})_6$ .<sup>40</sup> Furthermore, the formation of  $(\text{CpNiC}_4\text{H}_4)_2\text{Cr}_2(\text{CO})_4$  (4S-1) by disproportionation of  $(\text{CpNiC}_4\text{H}_4)_2\text{Cr}_2(\text{CO})_5$  (5T-1) into 4S-1 +  $(\text{CpNiC}_4\text{H}_4)_2\text{Cr}_2(\text{CO})_6$  (6S-1) is an exothermic process by 4.0 kcal/mol, while the disproportionation of  $(\text{CpNiC}_4\text{H}_4)_2\text{Cr}_2(\text{CO})_4$  (4S-1) into  $(\text{CpNiC}_4\text{H}_4)_2\text{Cr}_2(\text{CO})_5$  (5T-1) +  $(\text{CpNiC}_4\text{H}_4)_2\text{Cr}_2(\text{CO})_3$  (3Q-1) is an endothermic process by 10.7 kcal/mol (Table 4). These disproportionation energies also support the viability of  $(\text{CpNiC}_4\text{H}_4)_2\text{Cr}_2(\text{CO})_4$  (4S-1) as a synthetic objective.

#### 4. DISCUSSION

The two low-energy nickelacyclopentadienyl  $(\text{CpNiC}_4\text{H}_4)_2\text{Cr}_2(\text{CO})_6$  structures with Cr–Cr single bond distances of  $\sim 3.23$  Å are very similar to the experimental  $\text{Cp}_2\text{Cr}_2(\text{CO})_6$  structure with a Cr–Cr single bond distance of 3.281 Å.<sup>36</sup> The predicted *trans* configuration of the nickelacyclopentadienyl rings in the lowest energy  $(\text{CpNiC}_4\text{H}_4)_2\text{Cr}_2(\text{CO})_6$  structure 6S-1 is similar to the experimental *trans* configuration of the Cp rings in  $\text{Cp}_2\text{Cr}_2(\text{CO})_6$ .

The saturated  $(\text{CpNiC}_4\text{H}_4)_2\text{Cr}_2(\text{CO})_6$  structures 6S-1 and 6S-2 may be described as two  $(\text{CpNiC}_4\text{H}_4)\text{Cr}(\text{CO})_3$  radicals joined by the Cr–Cr bond. Unlike the corresponding  $\text{Cp}_2\text{Cr}_2(\text{CO})_n$  systems, the identity of these  $(\text{CpNiC}_4\text{H}_4)\text{Cr}(\text{CO})_3$  radicals is maintained in a series of unsaturated  $(\text{CpNiC}_4\text{H}_4)_2\text{Cr}_2(\text{CO})_n$  ( $n = 5, 4, 3$ ) structures formed by CO losses from  $(\text{CpNiC}_4\text{H}_4)_2\text{Cr}_2(\text{CO})_6$ . In this sense the  $(\text{CpNiC}_4\text{H}_4)\text{Cr}(\text{CO})_3$  radical can be considered to be a *bulky pseudohalogen radical*. Such structures are energetically competitive with more conventional  $(\text{CpNiC}_4\text{H}_4)_2\text{Cr}_2(\text{CO})_n$  structures resembling the corresponding  $\text{Cp}_2\text{Cr}_2(\text{CO})_n$  structures. The lowest energy  $(\text{CpNiC}_4\text{H}_4)_2\text{Cr}_2(\text{CO})_5$  structure 5T-1 (Figure 4) is a structure of this type. Thus, in 5T-1 a  $(\text{CpNiC}_4\text{H}_4)\text{Cr}(\text{CO})_3$  unit is bonded to a  $(\text{CpNiC}_4\text{H}_4)\text{Cr}(\text{CO})_2$  unit, mainly through a Cr–Cr single bond of length 2.738 Å, thereby giving the chromium atom in the  $(\text{CpNiC}_4\text{H}_4)\text{Cr}(\text{CO})_2$  unit only a 16-electron configuration. This lowest energy  $(\text{CpNiC}_4\text{H}_4)_2\text{Cr}_2(\text{CO})_5$  structure 5T-1 is a high-spin triplet structure with most of the spin density on the chromium atom with a 16-electron configuration (Figure S1). In 5T-1 two of the three CO groups of the  $(\text{CpNiC}_4\text{H}_4)\text{Cr}(\text{CO})_3$  unit become weakly semibridging CO groups with long Cr–C distances of 2.484 and 2.630 Å. A higher energy singlet  $(\text{CpNiC}_4\text{H}_4)_2\text{Cr}_2(\text{CO})_5$  structure, 5S-2, at  $\sim 10$  kcal/mol in energy above 5T-1 has a symmetrical distribution of four terminal CO groups and a single symmetrical bridging CO group across a formal Cr=Cr double bond of length 2.622 Å. Structure 5S-2, unlike 5T-1, has the favored 18-electron configuration for each chromium atom consistent with the singlet spin state.

The cyclopentadienyl structure  $\text{Cp}_2\text{Cr}_2(\text{CO})_4$ , with a formal short Cr≡Cr triple bond of length  $\sim 2.24$  Å and two semibridging CO groups, is known to be a very favorable species that can be synthesized by a simple thermal reaction of  $\text{Cr}(\text{CO})_6$  with a suitable cyclopentadiene derivative.<sup>6–8</sup> The lowest energy  $(\text{CpNiC}_4\text{H}_4)_2\text{Cr}_2(\text{CO})_4$  structure 4S-1 is a

structure exactly analogous with a predicted  $\text{Cr}\equiv\text{Cr}$  distance of  $\sim 2.27$  Å and long semibridging Cr–C distances of 2.573 Å to the two semibridging CO groups. However, the higher energy higher spin state  $(\text{CpNiC}_4\text{H}_4)_2\text{Cr}_2(\text{CO})_4$  structures 4Q-2 and 4T-3 at 10.0 and 12.6 kcal/mol, respectively, above 4S-1 can be formulated as  $(\text{CpNiC}_4\text{H}_4)\text{Cr}(\text{CO})_3$  units bonded to  $(\text{CpNiC}_4\text{H}_4)\text{Cr}(\text{CO})$  units, mainly through a Cr–Cr single or double bond for 4Q-2 and 4T-3, respectively. Again, pseudohalogen behavior of the  $(\text{CpNiC}_4\text{H}_4)\text{Cr}(\text{CO})_3$  unit is indicated. Structures 4Q-2 and 4T-3, like 5T-1, have two weakly semibridging CO groups from the  $(\text{CpNiC}_4\text{H}_4)\text{Cr}(\text{CO})_3$  unit to the  $(\text{CpNiC}_4\text{H}_4)\text{Cr}(\text{CO})$  unit. The spin densities in these structures lie on the  $(\text{CpNiC}_4\text{H}_4)\text{Cr}(\text{CO})$  chromium atom, consistent with the 14- or 16-electron configuration of this chromium atom.

The three lowest energy  $(\text{CpNiC}_4\text{H}_4)_2\text{Cr}_2(\text{CO})_3$  structures can be analogously dissected into  $(\text{CpNiC}_4\text{H}_4)\text{Cr}(\text{CO})_3$  +  $(\text{CpNiC}_4\text{H}_4)\text{Cr}$  units, again suggesting pseudohalogen behavior for the  $(\text{CpNiC}_4\text{H}_4)\text{Cr}(\text{CO})_3$  unit. These three structures represent the three different spin states, namely, quintet (3Q-1), triplet (3T-2), and singlet (3S-3), in ascending energy order, while having closely related geometries. All three  $(\text{CpNiC}_4\text{H}_4)_2\text{Cr}_2(\text{CO})_3$  structures have three semibridging CO groups from the  $(\text{CpNiC}_4\text{H}_4)\text{Cr}(\text{CO})_3$  unit to the  $(\text{CpNiC}_4\text{H}_4)\text{Cr}$  unit, with the long Cr–C distances ranging from 2.245 Å in 3S-3 to 2.455 Å in 3Q-1. Again the spin densities for the quintet and triplet  $(\text{CpNiC}_4\text{H}_4)_2\text{Cr}_2(\text{CO})_3$  structures lie almost entirely on the chromium atoms in the  $(\text{CpNiC}_4\text{H}_4)\text{Cr}$  units. Triply semibridged  $\text{Cp}_2\text{Cr}_2(\text{CO})_3$  structures were predicted by DFT several years ago.<sup>41</sup> However, the latter  $\text{Cp}_2\text{Cr}_2(\text{CO})_3$  structures do not have the semibridging CO groups oriented in the same direction, in contrast to all three  $(\text{CpNiC}_4\text{H}_4)_2\text{Cr}_2(\text{CO})_3$  structures here, which have all three semibridging CO groups oriented in the same direction.

In summary, all four  $(\text{CpNiC}_4\text{H}_4)_2\text{Cr}_2(\text{CO})_n$  systems have low-energy structures that can be dissected into  $(\text{CpNiC}_4\text{H}_4)\text{Cr}(\text{CO})_3$  +  $(\text{CpNiC}_4\text{H}_4)\text{Cr}(\text{CO})_{n-3}$  units with weakly semibridging CO groups from the  $(\text{CpNiC}_4\text{H}_4)\text{Cr}(\text{CO})_3$  unit to the  $(\text{CpNiC}_4\text{H}_4)\text{Cr}(\text{CO})_{n-3}$  unit. Such dissections suggest *pseudohalogen* behavior for the  $(\text{CpNiC}_4\text{H}_4)\text{Cr}(\text{CO})_3$  unit, with the dimer  $(\text{CpNiC}_4\text{H}_4)_2\text{Cr}_2(\text{CO})_6$  (6S-1 or 6S-2) being the pseudohalogen analogue of the free halogen  $\text{X}_2$  ( $\text{X} = \text{F}, \text{Cl}, \text{Br}, \text{I}$ ). The lowest energy such structures can be high-spin triplet or quintet structures reflecting a 14- or 16-electron configuration of the  $(\text{CpNiC}_4\text{H}_4)\text{Cr}(\text{CO})_{n-3}$  chromium atom rather than the favored 18-electron configuration. Only for the tetracarbonyl  $(\text{CpNiC}_4\text{H}_4)_2\text{Cr}_2(\text{CO})_4$  does a structure with a formal  $\text{Cr}\equiv\text{Cr}$  triple bond analogous to the stable  $\text{Cp}_2\text{Cr}_2(\text{CO})_4$  structure lie in energy below an isomeric structure dissected into  $(\text{CpNiC}_4\text{H}_4)\text{Cr}(\text{CO})_3$  +  $(\text{CpNiC}_4\text{H}_4)\text{Cr}(\text{CO})$  units. The lowest energy structures in the other  $(\text{CpNiC}_4\text{H}_4)_2\text{Cr}_2(\text{CO})_n$  systems ( $n = 6, 5, 3$ ) are all of types that can be dissected into  $(\text{CpNiC}_4\text{H}_4)\text{Cr}(\text{CO})_3$  +  $(\text{CpNiC}_4\text{H}_4)\text{Cr}(\text{CO})_{n-3}$  units.

## ■ ASSOCIATED CONTENT

### ■ Supporting Information

Figures S1–S3 showing the spin densities for the triplet  $(\text{CpNiC}_4\text{H}_4)_2\text{Cr}_2(\text{CO})_5$  structure 5T-1, the quintet and triplet  $(\text{CpNiC}_4\text{H}_4)_2\text{Cr}_2(\text{CO})_4$  structures, and the quintet and triplet  $(\text{CpNiC}_4\text{H}_4)_2\text{Cr}_2(\text{CO})_3$  structures, Tables S1–S4 showing the metal–metal distances (Å), total energies ( $E$ , hartrees), relative

energies ( $\Delta E$ , kcal/mol), zero-point energies (ZPEs), enthalpies ( $\Delta H$ ), free energies ( $\Delta G$ , kcal/mol), and spin expectation values  $\langle S^2 \rangle$  for the  $(\text{CpNiC}_4\text{H}_4)_2\text{Cr}_2(\text{CO})_n$  ( $n = 6, 5, 4, 3$ ) structures predicted by the M06-L and BP86 methods, Tables S5–S14 showing the atomic coordinates of the optimized structures for all structures, and complete Gaussian reference (ref 31). The Supporting Information is available free of charge on the ACS Publications website at DOI: 10.1021/acs.inorgchem.5b00362.

## ■ AUTHOR INFORMATION

### Corresponding Authors

\*E-mail: fenghao@mail.xhu.edu.cn.

\*E-mail: rbking@chem.uga.edu.

### Notes

The authors declare no competing financial interest.

## ■ ACKNOWLEDGMENTS

This research was supported by the National Natural Science Foundation of China (Grant 21403170), Chunhui Plan of the Ministry of Education of China (Grant Z2014063), Great Cultivating Project of the Education Department of Sichuan Province (15CZ0014), Innovation Foundation of Postgraduate of Xihua University, Youth Innovation Team of the Education Department of Sichuan Province (Grant No. 14TD0013 – China), and U.S. National Science Foundation (Grants CHE-1057466, CHE-1054286, and CHE-1361178).

## ■ REFERENCES

- (1) Piper, T. S.; Wilkinson, G. J. *Inorg. Nucl. Chem.* **1956**, 3, 104–124.
- (2) Fischer, E. O.; Hafner, W.; Stahl, H. O. *Z. Anorg. Allg. Chem.* **1955**, 282, 47–62.
- (3) Wilkinson, G. J. *Am. Chem. Soc.* **1954**, 76, 209–211.
- (4) King, R. B.; Bisnette, M. B. *J. Organomet. Chem.* **1967**, 8, 287–297.
- (5) Huang, J. S.; Dahl, L. F. *J. Organomet. Chem.* **1983**, 243, 57–68.
- (6) Curtis, M. D.; Butler, W. M. *J. Organomet. Chem.* **1978**, 155, 131–145.
- (7) King, R. B.; Efraty, A.; Douglas, W. M. *J. Organomet. Chem.* **1973**, 60, 125–137.
- (8) Potenza, J.; Giordano, P.; Mastropaolo, D.; Efraty, A. *Inorg. Chem.* **1974**, 13, 2540–2544.
- (9) Buchalski, P.; Grabowska, I.; Kaminska, E.; Suwińska, K. *Organometallics* **2008**, 27, 2346–2349.
- (10) Buchalski, P.; Grabowska, I.; Karaskiewicz, A.; Suwińska, K.; Jerzykiewicz, L. *Organometallics* **2008**, 27, 3316–3319.
- (11) Buchalski, P.; Jadach, P.; Pietrzykowski, A.; Suwińska, K.; Jerzykiewicz, L.; Sadlo, J. *Organometallics* **2008**, 27, 3618–3621.
- (12) Buchalski, P.; Zbierzna, J.; Suwińska, K. *Inorg. Chem. Commun.* **2009**, 12, 29–31.
- (13) Buchalski, P.; Kamińska, E.; Piwowar, K.; Suwińska, K.; Jerzykiewicz, L.; Rossi, F.; Laschi, F.; de Biani, F. F.; Zanello, P. *Inorg. Chem.* **2009**, 48, 4934–4941.
- (14) Colbran, S. B.; Robinson, B. H.; Simpson, J. *Organometallics* **1985**, 4, 1594–1601.
- (15) Brynda, M.; Gagliardi, L.; Widmark, P. O.; Power, P. P.; Roos, B. O. *Angew. Chem., Int. Ed.* **2006**, 45, 3804–3807.
- (16) Sieffert, N.; Bühl, M. *J. Am. Chem. Soc.* **2010**, 132, 8056–8070.
- (17) Schyman, P.; Lai, W.; Chen, H.; Wang, Y.; Shaik, S. *J. Am. Chem. Soc.* **2011**, 133, 7977–7984.
- (18) Adams, R. D.; Pearl, W. C.; Wong, Y. O.; Zhang, Q.; Hall, M. B.; Walensky, J. R. *J. Am. Chem. Soc.* **2011**, 133, 12994–12997.
- (19) Lonsdale, R.; Olah, J.; Mulholland, A. J.; Harvey, J. N. *J. Am. Chem. Soc.* **2011**, 133, 15464–15474.

- (20) Crawford, L.; Cole-Hamilton, D. J.; Drent, E.; Bühl, M. *Chem.—Eur. J.* **2014**, *20*, 13923–13926.
- (21) Zhekova, H.; Krykunov, M.; Autschbach, J.; Ziegler, T. *J. Chem. Theory Comput.* **2014**, *10*, 3299–3307.
- (22) Becke, A. D. *Phys. Rev. A* **1988**, *38*, 3098–3100.
- (23) Perdew, J. P. *Phys. Rev. B* **1986**, *33*, 8822–8824.
- (24) Feng, X.; Gu, J.; Xie, Y.; King, R. B.; Schaefer, H. F. *J. Chem. Theory Comput.* **2007**, *3*, 1580–1587.
- (25) Zhao, S.; Liu, Z. P.; Wang, W. N.; Fan, K.; Xie, Y.; Schaefer, H. F. *J. Chem. Phys.* **2006**, *124*, 184102–184111.
- (26) Zhao, Y.; Truhlar, D. G. *Theor. Chem. Acc.* **2008**, *120*, 215–241.
- (27) Huzinaga, S. *J. Chem. Phys.* **1965**, *42*, 1293–1302.
- (28) Dunning, T. H. *J. Chem. Phys.* **1970**, *53*, 2823–2833.
- (29) Wachters, A. J. H. *J. Chem. Phys.* **1970**, *52*, 1033–1036.
- (30) Hood, D. M.; Pitzer, R. M.; Schaefer, H. F. *J. Chem. Phys.* **1979**, *71*, 705–712.
- (31) Gaussian 09, revision A.02: Frisch, M. J., et al., Gaussian, Inc., Wallingford CT, 2009 (see the Supporting Information for full details).
- (32) Papas, B. N.; Schaefer, H. F. *J. Mol. Struct.* **2006**, *768*, 175–181.
- (33) NBO 5.0: Glendening, E. D.; Badenhoop, J. K.; Reed, A. E.; Carpenter, J. E.; Bohmann, J. A.; Morales, C. M.; Weinhold, F., Theoretical Chemistry Institute, University of Wisconsin, Madison, WI, 2001.
- (34) Reed, A. E.; Curtiss, L. A.; Weinhold, F. *Chem. Rev.* **1988**, *88*, 899–926.
- (35) Wiberg, K. B. *Tetrahedron* **1968**, *24*, 1083–1096.
- (36) Adams, R. D.; Collins, D. E.; Cotton, F. A. *J. Am. Chem. Soc.* **1974**, *96*, 749–754.
- (37) Zeng, Y.; Wang, S. J.; Feng, H.; Xie, Y.; King, R. B.; Schaefer, H. F. *New J. Chem.* **2011**, *35*, 920–929.
- (38) Jonas, V.; Thiel, W. *J. Chem. Phys.* **1995**, *102*, 8474–8484.
- (39) Silaghi-Dumitrescu, I.; Bitterwolf, T. E.; King, R. B. *J. Am. Chem. Soc.* **2006**, *128*, 5342–5343.
- (40) Sunderlin, L. S.; Wang, D.; Squires, R. R. *J. Am. Chem. Soc.* **1993**, *115*, 12060–12070.
- (41) Zhang, X.; Li, Q.; Xie, Y.; King, R. B.; Schaefer, H. F. *Dalton Trans.* **2008**, *35*, 4805–4810.